REPORT DOCUMENTATION PAGE

Form Approved
OMB No. 0704-0188

1. REPORT DATE *(DD-MM-YYYY)*	**2. REPORT TYPE**	**3. DATES COVERED** *(From - To)*
09-06-2017	Journal Article	

4. TITLE AND SUBTITLE
The physiology and toxicology of acute inhalation phosphine poisoning in conscious male rats

5a. CONTRACT NUMBER

5b. GRANT NUMBER

5c. PROGRAM ELEMENT NUMBER

6. AUTHOR(S)
Wong, B, Lewandowski, R, Tressler, J, Sherman, K, Andres, J, Devorak, J, Rothwell, C, Hamilton, T, Hoard-Fruchey, H, Sciuto, AM

5d. PROJECT NUMBER

5e. TASK NUMBER

5f. WORK UNIT NUMBER

7. PERFORMING ORGANIZATION NAME(S) AND ADDRESS(ES)

US Army Medical Research Institute of
Chemical Defense
8350 Ricketts Point Road
Aberdeen Proving Ground, MD
21010-5400

8. PERFORMING ORGANIZATION REPORT NUMBER

USAMRICD-P17-008

9. SPONSORING / MONITORING AGENCY NAME(S) AND ADDRESS(ES)
National Institutes of Health
National Institute of Allergy & Infectious Diseases
5601 Fishers Lane
Bethesda, MD 20892

10. SPONSOR/MONITOR'S ACRONYM(S)
NIAID

11. SPONSOR/MONITOR'S REPORT NUMBER(S)

12. DISTRIBUTION / AVAILABILITY STATEMENT

Approved for public release; distribution unlimited

13. SUPPLEMENTARY NOTES
Published in Inhalation Toxicology, 29(11),494-505, 2017. This work was supported by an interagency agreement between the NIH/NIAID and USAMRICD (IAA# AOD16027–001-00000).

14. ABSTRACT
See reprint.

15. SUBJECT TERMS
Inhalation exposure; Phosphine; Respiratory dynamics; Genomics; Metabolic poison

16. SECURITY CLASSIFICATION OF:			**17. LIMITATION OF ABSTRACT**	**18. NUMBER OF PAGES**	**19a. NAME OF RESPONSIBLE PERSON**
a. REPORT	**b. ABSTRACT**	**c. THIS PAGE**			Benjamin Wong
UNCLASSIFIED	UNCLASSIFIED	UNCLASSIFIED	UNLIMITED	29	**19b. TELEPHONE NUMBER** *(include area code)* 410-436-9649

HHS Public Access

Author manuscript

Inhal Toxicol. Author manuscript; available in PMC 2018 December 28.

Published in final edited form as:

Inhal Toxicol. 2017 September ; 29(11): 494–505. doi:10.1080/08958378.2017.1406564.

The Physiology and Toxicology of Acute Inhalation Phosphine Poisoning in Conscious Male Rats

Benjamin Wong, **Rebecca Lewandowski**, **Justin Tressler**, **Katherine Sherman**, **Jaclynn Andres**, **Jennifer Devorak**, **Cristin Rothwell**, **Tracey Hamilton**, **Heidi Hoard-Fruchey**, and **Alfred M. Sciuto**

Medical Toxicology Research Division, US Army Medical Research Institute of Chemical Defense, 2900 Ricketts Point Road, Aberdeen Proving Ground, MD 21010.

Abstract

Phosphine (PH_3) is a toxidrome-spanning chemical that is widely used as an insecticide and rodenticide. Exposure to PH_3 causes a host of target organ and systemic effects, including oxidative stress, cardiopulmonary toxicity, seizure-like activity, and overall metabolic disturbance.

A custom dynamic inhalation gas exposure system was designed for the whole-body exposure of conscious male Sprague-Dawley rats (250–350 g) to PH_3. An integrated plethysmography system was used to collect respiratory parameters in real-time before, during, and after PH_3 exposure. At several time points post-exposure, rats were euthanized, and various organs were removed and analyzed to assess organ and systemic effects. The 24 hr post-exposure LCt_{50}, determined by probit analysis, was 23,270 ppm×min (32,345 mg×min/m^3).

PH_3 exposure affects both pulmonary and cardiac function. Unlike typical pulmonary toxicants, PH_3 induced net increases in respiration during exposure. Gross observations of the heart and lungs of exposed rats suggested pulmonary and cardiac tissue damage, but histopathological examination showed little to no observable pathologic changes in those organs. Gene expression studies indicated alterations in inflammatory processes, metabolic function, and cell signaling, with particular focus in cardiac tissue. Transmission electron microscopy examination of cardiac tissue revealed ultrastructural damage to both tissue and mitochondria.

Altogether, these data reveal that in untreated, un-anesthetized rats, PH_3 inhalation induces acute cardiorespiratory toxicity and injury, leading to death, and that it is characterized by a steep dose-response curve. Continued use of our interdisciplinary approach will permit more effective identification of therapeutic windows and development of rational medical countermeasures and countermeasure strategies.

Keywords

Inhalation exposure; Phosphine; Respiratory dynamics; Genomics; Metabolic poison

Corresponding author: Benjamin Wong, Medical Toxicology Research Division, US Army Medical Research Institute of Chemical Defense, 2900 Ricketts Point Road, Aberdeen Proving Ground, MD, 21010-5400, Tel: 410.436.9649, ORCID: 0000-0001-6593-278X, Benjamin.j.wong.civ@mail.mil.

Disclosures

The authors report no conflicts of interest.

Introduction

Background

First discovered in the late eighteenth century and used as a fumigant since the 1930s, phosphine (PH_3) is a highly effective insecticide and rodenticide that now plays a vital role in global food security (Ryan and De Lima 2014). Metal phosphide (AlP, Mg_3P_2, Zn_3P_2) tablets rapidly degrade into colorless, odorless PH_3 gas upon contact with acid or water, are easy and inexpensive to obtain, and do not leave behind environmentally toxic residues, leading to its extensive worldwide use in the agricultural sector (Nath et al. 2011). Based on a 2014 report, between 2006 and 2010, approximately 372 tons of phosphides were used in four Californian counties alone to protect fruits, nuts, and grains (Reeve 2014). PH_3 gas is also widely used in the synthesis of complex chemicals (Berners-Price and Sadler 1988) and as a dopant for silicon semiconductor and photovoltaic process applications (Wang et al. 2005). In addition, PH_3 is a by-product of various metallurgical processes (Perkins, Wong, Olivera, et al. 2015) and illegal methamphetamine manufacture (Burgess 2001, Willers-Russo 1999). Human exposure to PH_3 typically occurs via inhalation as a result of improper use or accidental release of the fumigant (Proudfoot 2009).

PH_3 is a toxidrome-spanning chemical that shares many commonalities with pulmonary toxicants, metabolic poisons, blood agents, and cholinergics. Exposure to PH_3 causes a host of target organ and systemic effects, including cardiotoxicity, GI and pulmonary toxicity, hepatic damage, neurological toxicity, circulatory failure, electrolyte imbalance, cellular poisoning, oxidative stress, and overall metabolic disturbance (Anand et al. 2011, Nath, Bhattacharya, Tuck, Schlipalius and Ebert 2011, Perkins, Wong, Olivera and Sciuto 2015, Proudfoot 2009, Sciuto et al. 2016). The exact mechanism of PH_3 toxicity is purported to be inhibition of cytochrome *c* oxidase, but the extent of *in vivo* inhibition is species-dependent (Chefurka et al. 1976, Dua and Gill 2004, Jian et al. 2000, Nakakita 1987, Singh et al. 2006). However, the symptoms of phosphine exposure do not align with traditional toxic inhibitors of cytochrome *c* oxidase, thus indicating other toxic mechanisms. Literature reviews of data from metal phosphide ingestion and PH_3 gas inhalation in animal models and human exposures implicate altered mitochondrial physiology, metabolic rates, and oxidative stress as central elements of PH_3 toxicity (Nath, Bhattacharya, Tuck, Schlipalius and Ebert 2011, Sciuto, Wong, Martens, Hoard-Fruchey and Perkins 2016). Human victims of PH_3 poisoning present with diverse, non-specific symptoms, rendering accurate diagnosis in the absence of *a priori* knowledge particularly challenging. Human mortality rates are high, typically exceeding 60–70% (Proudfoot 2009), and current methods of detecting PH_3 in victims are ineffective and subject to false positives (Proudfoot 2009, Raina et al. 2003). In addition, the relative ease of obtaining and using phosphides render them a security concern which is compounded by the lack of rigorous scientific research into medical treatment for PH_3 exposure, currently limited to supportive care (Bogle et al. 2006, Mehrpour et al. 2012, Proudfoot 2009).

The study described herein was designed to address some of the previously unexplored and undescribed aspects of PH_3 poisoning using an interdisciplinary approach. We combined toxicological, biochemical, physiological, genomic and histopathologic evaluations to

develop an exposure model to characterize toxicity. The two-phase project consisted of a model development and validation phase, which included the initial evaluation of signs and symptoms of PH_3 toxicity and LCt_{50} assessment, followed by an experimental dosing phase, which centered on examining the dose-dependency of physiological and biochemical effects following inhalation PH_3 exposure. To replicate a potential human exposure scenario while maximizing physiological data collection, we developed a gas inhalation model to account for the most likely route of exposure and combined it with a paradigm utilizing individually exposed, unrestrained animals within physiological monitoring chambers. The applicability of Haber's Rule to phosphine in a high concentration, short exposure dose regime was assessed through the determination of an LCt_{50} and analysis of real-time respiratory and cardiac function data. Further characterization of toxicity was accomplished using traditional and ultrastructural histopathology and the first ever genomic analysis in PH_3 gas-exposed animals. Our approach, model, and data contribute valuable information toward understanding molecular mechanisms of toxicity. More importantly, this study establishes the baseline for further research efforts aimed at identifying therapeutic windows, the testing of medical countermeasures, and the development of rational medical countermeasure strategies for addressing inhalation PH_3 exposure.

Materials and Methods

Chemicals and Exposure System Configuration

A custom dynamic exposure system was used to expose conscious, unrestrained animals to PH_3 gas (compressed PH_3 gas, ≥97% pure, 10% PH_3 in N_2, Custom Gas Solutions LLC, Durham, NC, USA) or filtered room air (Figure 1 – Exposure System Schematic). All PH_3 exposures were performed in a custom-designed glove box (The Baker Company, Sanford, ME) and with appropriate personal protective equipment for the handling of toxic industrial chemicals (TICs). The system consisted of a gas mixing and metering system connected to six exposure chambers (two control and four PH_3-exposed operating in parallel) with integrated real-time physiological monitoring capabilities. Gas mixtures of various concentrations were generated by combining PH_3 gas metered by pressure (P-602CV-6K0A-RAD-22-K; Bronkhorst USA Inc.; Bethlehem, PA, USA) and mass (F-201CV-500-RAD-22-K; Bronkhorst USA Inc.; Bethlehem, PA, USA) flow controllers with filtered room air from an air compressor (OF302–25M; JUN-AIR/Gast Manufacturing, Inc.; Benton Harbor, MI, USA) metered by a mass flow controller. The resulting PH_3 concentrations were assessed using an in-line Fourier transform infrared spectroscopy (FTIR) gas analyzer (CR-1000; Gasmet Technologies Inc.; Toronto, ON, CA). PH_3 gas mixtures were then fed through a custom-designed air manifold connected to four whole-body exposure chambers. Exposure chambers were modified whole-body plethysmography (WBP) units (FinePointe Series Whole Body Plethysmography Rat Chamber; Data Sciences International; St. Paul, MN, USA) capable of simultaneously permitting gas entry and continuous collection of respiratory parameters before, during, and after exposure. Bias flow generators (Bias Flow Fresh Air Pump; Data Sciences International; St. Paul, MN, USA) connected to the WBP chambers generated a slight vacuum to withdraw gas from the manifold into the chamber, ensuring agent flow to each exposure unit at physiologically compatible rates. Exit flows

from the manifolds and bias flow units were passed through an activated charcoal decontamination unit.

PH_3 exposure doses were expressed as the concentration-time (*Ct*) product of the average PH_3 concentration of the gas mixture ($\bar{C}_{exp}$, in ppm) and the experimental exposure time (t_{exp}, in min) in ppm×min units. Under typical experimental conditions (25°C, 1 atm), the conversion from ppm to mg/m^3 is achieved by multiplying $\bar{C}_{exp}$ in ppm by 1.39 (Ideal Gas Law, simplified to [C, mg/m_3] = [C, ppm] × MW/24.45, where MW is the molecular weight of PH_3, or 33.99758 g/mol).

Animal Experimentation

All research was conducted in compliance with the Animal Welfare Act and other federal statutes and regulations relating to animals and experiments involving animals. It adhered to principles stated in the Guide for the Care and Use of Laboratory Animals, National Research Council, published by the National Academy Press, 2010, and the Animal Welfare Act of 1966, as amended. The study protocol was approved by the Institutional Animal Care and Use Committee, United States Army Medical Research Institute of Chemical Defense (USAMRICD), Aberdeen Proving Ground, MD.

Male Sprague-Dawley rats (300–400 g, Charles River Laboratories, Wilmington, MA) were housed individually under standard conditions with a 12 hr light/dark cycle and standard rat chow and water available *ad libitum*. For exposures, animals were individually placed into WBP chambers 20 min before the start of exposure ($t = -20$ min) and permitted to acclimate for 10 min (Figure 2 – Inhalation Exposure Paradigm). At 10 min prior to the start of exposure ($t = -10$ min), baseline respiratory dynamics were recorded until the start of exposure. At the initiation of exposure ($t = 0$ min), flow of the PH_3 gas mixture into each exposure chamber began and continued for 10 to 40 min (t_{exp}). At the end of exposure, animals remained in the WBP for an additional 10 min off-gassing period. Real-time respiratory parameters were collected continuously during each of these time intervals. At the conclusion of the off-gassing period ($t = t_{exp}+10$ min), surviving animals were returned to their cages and observed until their predetermined endpoint of 1, 3, 6, or 24 hr. Animals were then deeply anesthetized using an intramuscular injection of ketamine (90 mg/kg) in combination with xylazine (10 mg/kg) and euthanized via exsanguination. For histopathological examination, anesthetized animals were transcardially perfused with phosphate-buffered saline (PBS) followed by a fixative solution of 10% neutral-buffered formalin. Heart, lungs, kidneys, liver, and brain tissues were then immersion-fixed in 10% neutral-buffered formalin for 3 days before being processed to paraffin. For biochemical and genomic assays, the heart, lung, kidney, liver, and brain tissue of anesthetized animals were removed, flash frozen in liquid N_2, and stored at −80°C until processed.

Clinical Observations

All animals were monitored for clinical signs of PH_3 intoxication prior to, during, and following exposure. The primary symptoms observed included excitability, lethargy, and ataxia. General appearance, movement, and natural behavior were also observed, and

deviations in these parameters from controls were recorded as potential symptoms of PH_3 exposure.

Respiratory Dynamics Data Collection and Analysis

Each exposure/WBP unit was modified to permit introduction of PH_3 gas without impacting existing connections, data collection devices, or their integrity. Specialized software (FinePointe Software v2.3.1.16, Data Sciences International, St. Paul, MN, USA) and customized routines were used to collect respiratory dynamics data in real time for multiple time periods. Parameters included respiratory frequency (*f*), and minute and tidal volume (MV, TV). All raw data were exported and analyzed using custom-designed programs (Microsoft Visual Basic for Applications v7.0.1639; Microsoft Corporation; Redmond, WA, USA), spreadsheet software (Microsoft Excel v14.1.7166.5000 [32-bit]; Microsoft Corporation; Redmond, WA, USA), and statistical and graphing software (GraphPad Prism v5.04; GraphPad Software, Inc.; La Jolla, CA, USA). The normalizing value for each respiratory parameter was calculated as the average of all controls for that parameter over an exposure period of 40 min, which was the maximum exposure length for these studies (Table 1 – Baseline Values for Respiratory Dynamics Parameters). Bodyweight-affected parameters (TV, MV) were normalized to bodyweight and control averages. Elapsed time relative to exposure initiation (*t*) for each concentration-time product was normalized to its respective exposure length (t_{exp}), with $t_n = t/t_{exp}$. Graphs of respiratory parameters are shown as normalized respiratory parameter versus normalized time. For any particular parameter of interest, statistical analyses of the differences between the control- and PH_3-exposed animals at 24 hours post-exposure were performed using GraphPad Prism v5.04 (GraphPad Software Inc., San Diego, CA). As appropriate, one- or two-factor analysis of variance followed by Tukey's multiple comparison test or Bonferroni's correction was used. Probability (*p*) values less than or equal to 0.05 were considered statistically significant.

Equivalent Endpoint Analysis (Haber's Rule)

Haber's Rule and the Toxic Load Model of equivalence of effect (Flury 1921, Haber 1924, Pauluhn 2014, Ten Berge and van Heemst 1983, Ten Berge et al. 1986, Witschi 1999) are based on connecting exposure conditions to equivalent physiological endpoint. An equation in the form of $k = C^a t^b$, in which *k* is the equivalent physiological endpoint and concentration (*C*) and time (*t*) are the exposure conditions, was established to assess the application of both theories to PH_3 exposure. Exposure conditions were quantified by the calculated exposure equivalent (CEE, mg/kg) (Wong et al. 2013), which yields the time-dependent amount of PH_3 delivered to an animal over the course of exposure, expressed in mg of PH_3 per kg of body weight. The equivalent physiological endpoint was quantified by the accumulated volume (AV, mL). For CEE:

$$CEE = \int_0^{t_{exp}} \frac{MV(t) \times C(t) \times IF_A(t)}{m(t)} dt \quad (1)$$

in which the inhaled fraction, $IF_A(t)$, is assumed to be a constant value of 1 for gases. For a 20- to 40-minute exposure, animal mass (m, g) was considered to be time-independent, and agent concentration (C, mg/m^3) reached its maximum value rapidly enough such that it was also time-independent, allowing Equation 1 to simplify to:

$$CEE = \frac{\overline{C}}{\overline{m}} \int_0^{t_{exp}} MV(t)dt \quad (2)$$

wherein $\overline{C}$ and $\overline{m}$ are the average PH_3 concentration and average animal mass, respectively. AV is the total inhaled volume over a given time and was calculated from Equation 3:

$$AV = \int_0^{t_{exp}} MV(t)dt \quad (3)$$

and, to similarly scale the contributions of exposure concentration and time to the physiological endpoint, was described mathematically in the form of the Power Law (Ten Berge and van Heemst 1983, Ten Berge, Zwart and Appelman 1986):

$$AV = \breve{Q}\,\overline{C}^a t^b \quad (4)$$

in which $\breve{Q}$ is an empirically derived constant scaling the effects of concentration and exposure time on the physiological outcome, and no inherent assumptions are made about the relative influence of either concentration or exposure time, with both exponents a and b set as variables. Substituting Equation 4 into Equation 3 and then Equation 2,

$$CEE = \frac{\overline{C}}{\overline{m}} \breve{Q}\,\overline{C}^a t^b = \frac{\breve{Q}\,\overline{C}^{a+1} t^b}{\overline{m}} \quad (5)$$

$$CEE \times \overline{m} = \breve{Q}\,\overline{C}^{a+1} t^b \quad (6)$$

The parameters of interest here are the exponents of $\overline{C}$ and t. Taking the natural logarithm of Equation 6 and simplifying $a + 1 = a$, $\ln \breve{Q} = \breve{Q}$, and $\hat{k} = CEE \times \overline{m}$ yields:

$$\ln \hat{k} = a \ln \overline{C} + b \ln t + \breve{Q} \quad (7)$$

Equation 7 expresses the relationship of exposure conditions to physiological outcome and was used to derive Haber's Rule and Power Law equations for our PH_3 exposure system.

Routine and Ultrastructural Histopathology

For light microscopy, tissue samples embedded in paraffin were sectioned to 5–6 μm in thickness, mounted on glass slides, and stained with hematoxylin and eosin (H&E). A scale describing the amount of damaged tissue (0 = none; 1 = mild, 1–10%; 2 = moderate, 10–50%; 3 = severe, >50%) was used to score the heart, lungs, brain, kidney, and liver of exposed animals at multiple doses (0 to 40,000 ppm×min) across multiple time points post-exposure (1, 3, 6, and 24 hr post-exposure). For transmission electron microscopy (TEM), following transcardial perfusion and immersion fixation using 10% neutral buffered formalin, heart tissue from left ventricle was trimmed to appropriate size for TEM analysis and post-fixed using 0.1M sodium cacodylate buffered 1.6% paraformaldehyde/2.5% glutaraldehyde and 1% osmium tetroxide for 1 hr each. Tissues were then dehydrated through a series of graded ethanols, followed by resin infiltration using propylene oxide and Poly/Bed® 812 embedding media. Ultrathin tissue sections approximately 90 nm thick were mounted on copper mesh grids and counter-stained using uranyl acetate and lead citrate. Imaging was performed using a JEOL JEM-1400 transmission electron microscope.

Genomics

Total RNA was isolated using RNeasy Plus Mini Kits (QIAGEN; Germantown, MD, USA). RNA quality and quantity were determined using an Agilent 2100 Bioanalyzer (Agilent Technologies; Santa Clara, CA, USA) and a NanoDrop ND-1000 UV-Vis spectrophotometer (Thermo Fisher Scientific; Waltham, MD, USA), respectively. Samples were processed for hybridization using the GeneChip 3’ IVT PLUS Reagent Kit (Affymetrix) to amplify, biotinylate, and fragment complementary RNA (cRNA) from poly(A) RNA in total RNA samples according to manufacturer instructions (Affymetrix; Santa Clara, CA, USA). Labeled RNA was hybridized to GeneChip HT RG-230 PM Array Plates (Affymetrix) then scanned using the Affymetrix GeneTitan System. Raw signal intensities were imported into Partek Genomic Suite (v6.6 Partek Inc., St. Louis, MO, USA) and normalized using robust multi-array averaging (RMA). Principal component analysis (PCA) was used to identify patterns and major sources of variability in the data. Analysis of variance (ANOVA) was used to identify gene expression differences induced by PH_3 exposure (fold change ≥ 1.5 or ≤ −1.5; p-value ≤ 0.05). Probeset ID, fold change, and p-values were imported into Ingenuity Pathway Analysis (IPA; Qiagen Inc., Valencia, CA, USA) to map genes altered by PH_3 exposure to canonical pathways, biological functions, diseases and disorders, and gene networks.

Results

Toxic Response to Phosphine Exposure

Animals were exposed to control air or PH_3 at various concentration-time products ranging from 10,000 to 40,000 ppm×min (500 – 1000 ppm for 20 – 40 min) to determine an LCt_{50} at 24 hr (Supplemental Material, Table 3 – Probit Analysis Development). No lethality was observed in animals exposed to PH_3 at doses of 10,000 to 19,000 ppm×min. Lethality at 20,000 and 30,000 ppm×min was 43% and 67%, respectively, and no animals survived at 33,000 and 40,000 ppm×min. Probit analysis yielded a 24-hour LCt_{50} of 23,270 ppm×min (32,345 mg×min/m^3 at 25°C and 1 atm) (Figure 3 – Lethality of Inhaled Phosphine) with a

confidence interval of 20,767 to 26,075 ppm×min. Control animals did not show any overt signs of toxicity.

Signs of exposure to PH_3 were varied, and the most prominent were sporadic excitability, prolonged lethargy, and ataxia. These symptoms typically occurred in that order and were observed in both the model development and experimental phases at all doses except the lowest (10,000 ppm×min). Overall, increased excitability was observed during the first half of exposure ($t_n = 0 – 0.5$), with the majority of animals appearing lethargic by the exposure midpoint ($t_n = 0.5$). Animals remained lethargic throughout the remainder of exposure and through the offgas period ($t_n = 0.5 – 1.6$). Ataxia was also observed in this time period. Normalized time of death (t_{TODn}) for any animal that did not survive to its experimental endpoint in either phase of the project was calculated as the ratio of its time of death following the start of exposure (t_{TOD}) to its exposure length (t_{exp}), $t_{TODn} = t_{TOD}/t_{exp}$. The binned distribution of t_{TDDn} (Figure 4 – Time of Death Distribution) shows that 74% of all deaths occurred from $t_{TOD} = 0.4 – 1.6$, and most of the remainder by $t_{TOD} = 2.8$.

Other signs and symptoms of PH_3 exposure included licking, chewing, facial fasciculation, retching, increased and excessive defecation, coprophagy, tremors, convulsions, and loss of color in the ears and extremities. For the second set of symptoms, no dose-dependent correlation for either their presence or intensity could be established, and similarly, no dose-dependent or statistically significant body weight loss was observed over 24 hr in all animals exposed to PH_3. Although no set of observed symptoms could be correlated to outcome, the overwhelming majority of deaths were immediately preceded by convulsions that ranged from mild tremors to severe whole-body contortions — again, with no correlation between severity of convulsions and any prior clinical observations — followed by cessation of respiratory activity.

Respiratory Dynamics during Exposure

Parameters of respiratory function (f, MV, TV) were collected before, during, and after exposure to control air and various concentration-time products of PH_3. These inhaled exposure doses ranged from $0.4\times LCt_{50}$ to $1.6\times LCt_{50}$ and are summarized in Supplemental Material, Table 4, Experimental Dose Selection. Normalized parameters of respiratory dynamics versus normalized exposure time, including f_n, TV_n, and MV_n, are shown in Figure 5, Respiratory Dynamics during Exposure to Phosphine Gas.

Across all exposure doses, PH_3 induced an immediate increase in f_n, for which the magnitude was not dose-dependent. As exposure progressed, f_n gradually decreased but did not typically reach control values (Figure 5A, 5B). At all doses other than 10,000 ppm×min, TV_n sharply increased between $t_n = 0$ and 0.2, and remained elevated for the remainder of exposure. At 10,000 ppm×min (500 ppm × 20 min), TV_n was slightly affected, but the sharp and sustained increase was absent (Figure 5C and5E). At all doses other than 10,000 ppm×min, the general trend in MV_n during exposure was that it was substantially elevated as compared to controls (> 150%) from $t_n = 0.1 – 0.7$ and then less elevated (between 100% and 150%) from $t_n = 0.7 – 1.0$ (Figures 5E and5F). This increase was initially driven by an

elevated f_n from $t_n = 0$ to 0.2 before the sharp increase in TV_n became the dominating factor (Figures 5A to 5D).

Equivalent Endpoint Analysis

Respiratory dynamics data were used to calculate CEEs (Table 1), combined with Equation 7 ($\ln \hat{k} = a\ln \bar{C} + b\ln t + \breve{Q}$) and analyzed using nonlinear least squares regression to solve for the exponents of interest, a and b (Supplemental Material, Table 5). The final form of the equation for equivalent endpoint is thus:

$$CEE = \frac{0.004895}{m} C^{1.315} t^{1.473} \quad (8)$$

Equivalently, if Equation 7 is rearranged into the form of the Toxic Load model,

$$\ln \hat{k} = b\ln(C^n \times t) + \breve{Q} \quad (9)$$

where $n = a/b$, then the Toxic Load exponent has a value of 0.8938 ± 0.2436. Equation 9 still simplifies to a form in which t may have an exponent that is not equal to 1, rendering Equation 8 more instructive. If the base assumption inherent in the Toxic Load theory that concentration drives physiological endpoint is applied to PH_3 exposure, then the appropriate equation is a modified form of Equation 7, wherein $b = 1$ and rearrangement yields a simple linear relationship.

$$\ln \frac{\hat{k}}{t} = a\ln C + \breve{Q} \quad (10)$$

The final form of the simplified equation for equivalent endpoint derived from Equation 10 (Supplemental Material, Table 6) is thus:

$$CEE = \frac{0.1}{m} C^{1.010} t \quad (11)$$

Genomics

In the absence of physiological indicators of a tissue-specific toxicant, molecular evaluation of tissues was performed. Gene expression changes using microarray were assessed for heart, lung, kidney, liver, and brain tissue taken from animals exposed to 15,480 ppm×min of PH_3. Principal Component Analysis (PCA) of gene expression values indicated tissue type as the greatest source of variability in the dataset (Supplemental Material, Figure 9 – Principal Component Analysis by Tissue Type). When PCA was performed for individual tissues (Figure 6 – Principal Component Analysis of Cardiac Tissue), PH_3 exposure was identified as a major source of variability in the dataset. In cardiac tissue, transcriptional changes associated with immune response, inflammation, and metabolism were observed,

indicating organismal injury and cardiovascular aberrations. Temporal patterns of transcriptional changes in cardiac tissue indicate a progression of both inflammatory and metabolic canonical pathways and diseases and disorders. Molecular and cellular functional analysis indicates changes in cell death and survival as well as metabolism, suggesting injury to cardiac tissue in response to PH_3 exposure (Figure 7 – Canonical Pathway Analysis of Cardiac Tissue). Pathway analysis of gene expression changes induced by PH_3 in renal tissue revealed diseases and disorders and physiological system development and function changes related to the cardiovascular system, while in lung tissue, cardiovascular disease was the top disease and disorder (data not shown), indicating molecular changes affecting the cardiac tissue.

Routine and Ultrastructural Histopathology

Histological assessment of H&E stained tissues did not indicate any differences between time-matched controls and exposed animals. Average scores for all combinations of exposure dose and time points (0 to 40,000 ppm×min, Supplemental Material, Tables 3 and 4) for each organ ranged from 0.03 to 0.67, with no statistically significant differences present in any combination. Approximately 75% of all scores for each organ were 0. However, gene expression analysis indicated the strong likelihood of cardiac tissue damage, and the subsequent ultrastructural pathological analysis of the left ventricles of animals exposed to 15,480 ppm×min PH_3 revealed compromised mitochondria and structural damage (Figure 8 – Transmission Electron Microscopy of Cardiac Tissue). Edematous intermyofibrillar mitochondria with swollen and lysed cristae were present as early as 3 hr post-exposure. By 6 hr post-exposure, degenerated cardiac myofibers characterized by sarcomere striation pattern loss, myofilament loss, swollen mitochondria, large intermyofibrillar vacuoles, intermyofibrillar edema, and edematous endomysium were observed.

Discussion and Conclusions

Inhalation PH_3 studies in animal models are rare, and no other published results have investigated a high dose, acute exposure that would be more characteristic of an industrial accident. Commercial use recommendations for PH_3 fumigation range from 200 to 1,000 ppm (Cavasin et al. 2006, Tumambing et al. 2012) and encompass both PH_3 generated from metal phosphides and liquefied PH_3 gas. The few existing studies of inhalation PH_3 exposure in animals have concentrations below the low end of this range (< 200 ppm) combined with long and/or multiple exposures (> 1 hr) (Barbosa et al. 1994, Kligerman et al. 1994, Muthu et al. 1980, Newton et al. 1993). The source of PH_3 in these studies also differed: some generated PH_3 from metal phosphide tablets and others used pure PH_3 gas (Barbosa, Rosinova, Dempsey and Bonin 1994, Kligerman, Bishop, Erexson, Price, O'Connor, Morgan and Zeiger 1994, Newton, Schroeder, Sullivan, Busey and Banas 1993); each study also used a different exposure system characterized by unique operating conditions and geometries.

Herein, we describe an interdisciplinary approach to the development and characterization of a more comprehensive animal model for PH_3 inhalation that can form the basis for

systematically addressing several unknowns surrounding PH_3, including mechanism of action, the window for therapeutic intervention, and the identification of therapeutic targets for medical treatment. Our inhalation exposure model focused on the 387 to 1000 ppm range over 10 to 40 minutes to more closely mirror an accidental acute industrial exposure. In addition, a variety of analytical techniques and methods, including real-time physiological monitoring and genomic and histopathological analyses, were used to systematically quantify clinically relevant parameters of PH_3 exposure and provide mechanistic insights of PH_3 toxicity.

Agent Toxicity and Equivalent Endpoint Analysis

Inhalation PH_3 exposure is characterized by a steep probit slope of 11 (Figure 3), ranking it among chemical warfare nerve agents such as sarin, which has a probit slope in the 9.4 to 13.2 range (Mioduszewski et al. 2002). Such agents, for which toxicity is more dependent on exposure concentration than on exposure time, are often characterized by a narrow range of *Ct*s centered around the LCt_{50} in which exposure results in all exposed animals dying or all exposed animals living. This binary outcome was consistent with inhalation PH_3 exposure. However, the time-of-death curve for PH_3 (Figure 4) indicates that exposure outcome is also dependent on time, as the majority of animals died in a narrow window near the end of the exposure period, regardless of the exposure concentration or length. Additionally, the temporal development of PH_3 exposure symptoms was also observed to scale to total exposure time, with the initial onset, duration, and progression of intoxication occurring at similar normalized time points. These observations are not necessarily contradictory for a toxidrome-spanning chemical such as PH_3 since both concentration and time can be the primary driver of toxicity, albeit in different dose regimes, resulting in regime-specific exposure symptoms and timelines of development, a claim supported by our data.

An equivalent physiological endpoint analysis, in the form of Haber's Rule and its refinement, the Power Law, was used to quantitatively assess the relative roles of exposure concentration and time in inhalation PH_3 toxicity. When the complete form of the Power Law ($k = C^a \times t^b$), which does not *a priori* assume the importance of either concentration or time in an inhalation exposure, was used, a = 1.315 and b = 1.473, indicating slight deviations from linear dependence on both C and t with a slightly stronger scaling of physiological endpoint with time versus concentration. Simplifying the Power Law to assume stronger concentration scaling ($k = C^n \times t$) reinforces this idea, with the toxic load exponent ranging from 0.89 to 1.01, which effectively reduces to Haber's Rule ($k = C \times t$). The two different methods of deriving Toxic Load Exponents yield approximately equal exponents for both C and t when accumulated volume (AV) is used as the equivalent physiological endpoint. Thus, within the range of exposure doses tested, phosphine more closely follows Haber's Rule than the generalized Power Law. However, our data also indicate a scaling of physiological endpoint to exposure length and support the idea that PH_3 can follow Haber's Rule in high-dose regimes and the Power Law in low-dose regimes.

Other researchers have published data that are consistent with this argument, with one group calculating the toxic load exponent at n = 0.9 (Winks 1982, Winks 1984, Winks 1986) and another indicating that the toxicity of PH_3 is disproportionately enhanced when exposure

times are extended (Cheng et al. 2003). Supplemental Material, Table 7 summarizes observed lethal doses documented in other rat models in the limited inhalation PH_3 literature. While some of these models used repeat exposures and others used single exposures, all of them utilized low concentrations of PH_3 (10 – 33.3 ppm) for an extended period of time (up to 6 hr). The range of reported lethal doses (2,400 – 17,485 ppm×min) is substantially lower than our LCt_{50} of 23,270 ppm×min and supports the idea that a low dose of PH_3 over a long period of time can induce lethality at substantially lower *Ct* products when compared to a high concentration exposure. In these cases, however, the form of the Power Law that describes PH_3 would scale linearly with concentration but exponentially with time.

Respiratory Dynamics and General Observations during Exposure

Inhalation of PH_3 induced dose-dependent effects on respiratory function as measured by f_n, TV_n, and MV_n (Figure 5). Based on the general trends in these parameters, the exposure doses were broadly categorized as being low (10,000 ppm×min), moderate (15,480; 16,500 ppm×min) or high (21,250; 30,000; 37,400 ppm×min). At the low dose, the effects of PH_3 inhalation on respiratory dynamics and clinical observations were markedly different from those observed at all other exposure doses, with only slight increases in MV_n and no discernible signs and symptoms observed. However, the increase in net respiration was consistently observed at all PH_3 exposure doses, and this contrasts sharply with previous work using real-time plethysmography to examine the respiratory patterns of rats during exposure to chemical agents from different toxidromes, including diisopropylfluorophosphate (DFP) (Wong, Perkins, Santos, Rodriguez, Murphy and Sciuto 2013), soman (Perkins, Wong, Rodriguez, et al. 2015), and ammonia (Perkins et al. 2017), which found that agent exposure typically induced net decreases in respiration over the course of exposure. However, for PH_3, the elevation of MV is primarily driven by increases in TV at the moderate and high doses, but by increases in *f* in the low-dose group.

Further support for the dose-regime-dependent toxicological behavior described above in the Equivalent Endpoint Analysis is evident in the temporal development of the primary clinical observations characterizing PH_3 exposure. Similar to the respiratory effects, clinical observations manifest differently at the lowest dose (10,000 ppm×min), with no discernible signs of intoxication noted. Increasing *Ct* resulted in qualitatively dose-dependent decreases in the time to onset and the temporal spacing in between the major primary clinical observations (excitability, lethargy, ataxia) but did not dose-dependently affect their magnitude or intensity. This scaling is also consistent with our observations on the relative time of death in exposed animals (Figure 4).

Overall, these data support the proposed dose-regime dependent toxicological behavior described above in the Equivalent Endpoint Analysis, and improved quantification of these trends and events may be able to contribute to a quantitative method for triage of exposure victims, especially as research focus shifts toward potential countermeasures and countermeasure strategies.

Genomics

To investigate molecular mechanisms of phosphine toxicity, genomic analysis was conducted on several organs. Microarray analysis provided a roadmap to drive more in-depth experimentation toward a target tissue for PH_3 exposure. To our knowledge, this is the first genomic analysis following an inhalation PH_3 exposure. The PH_3-induced changes in gene expression revealed cardiac-specific alterations that indicated inflammation, organismal damage, and metabolic aberrations in the heart (Figure 7), all consistent with the hypothesis that PH_3 is a metabolic poison. In addition, renal tissue analysis revealed patterns of disease and function indicating cardiovascular system abnormalities, while transcriptional changes in lung tissue enriched disease pathways aligning closely with cardiovascular disease (data not shown). Combined, these findings suggest that the heart is a primary target of PH_3 toxicity and that the development of symptoms of PH3 toxicity and the symptoms themselves may originate from cardiac compromise.

Histopathological Analysis

Initial assessment of the primary target organ of PH_3 toxicity was complicated by the lack of histopathological findings. H&E staining did not indicate the presence of damage in the organs of animals that died from PH_3 exposure. The majority of these deaths occurred in close temporal proximity to the acute exposure (t_n = 1.0 – 1.6), and the lack of such findings indicated the need for a more discriminating histopathological assessment. Transmission electron microscopy (TEM), encouraged by the genomic analysis, was utilized to examine the ultrastructure of cardiac tissue.

Analysis of left ventricular tissue from exposed animals showed mitochondrial compromise and myofibril degeneration starting as early as 3 hr post-exposure (Figure 8), supporting findings from the genomic analysis. Exposed animals that survived to 6 hr typically survived to 24 hr, at which time they were bright, alert, and responsive. These animals showed little to no signs of exposure, which was surprising, given the substantial compromise of cardiac tissue integrity discovered in animals surviving to 6 hr post-exposure. While chronic effects were outside the scope of this research, these TEM images indicate the potential for long-term cardiac complications stemming from a single, acute PH_3 exposure.

Summary

This is the first study to utilize an interdisciplinary approach to characterize the toxicity of PH_3 in male rats through a combined analysis of physiology, histopathology, and genomics. Inhalation exposure to PH_3 in our whole-body, unrestrained, unanesthetized rat model induced marked changes in clinical observations, respiratory dynamics, histopathology, and gene expression. During exposure to PH_3 in the acute dose regime (high concentration, short duration), male rats exhibited elevated MVs throughout while also experiencing periods of sporadic excitability, prolonged lethargy, and ataxia. Gross observations of the heart and lungs of exposed rats suggested pulmonary and cardiac tissue damage, but histopathological examination showed little to no observable pathologic changes in those organs. Gene expression studies indicated alterations in inflammatory processes, metabolic function, and cell signaling, with particular focus in cardiac tissue. This transcriptional response

emphasizing the heart as a target organ prompted using transmission electron microscopy to examine cardiac tissue, which revealed ultrastructural damage to both tissue and mitochondria. Altogether, these data reveal that PH_3 is characterized by a steep dose-response curve and that inhalation induces acute cardiorespiratory toxicity and injury in untreated, unanesthetized rats.

The elucidation of many aspects of PH_3 poisoning has been achieved with our interdisciplinary approach, leading to a more comprehensive characterization of PH_3 toxicity and the potential for diagnostic and/or predictive models based on clinically assessable physiological parameters. Continued use of this flexible approach will permit more effective identification of therapeutic windows and development of rational medical countermeasures and countermeasure strategies.

Supplementary Material

Refer to Web version on PubMed Central for supplementary material.

Acknowledgements

The views, opinions, and findings contained herein are those of the authors and should not be construed as an official Department of Army position, policy, or decision unless so designated by other documentation. Special thanks to the Comparative Pathology Branch for providing outstanding pathology support. The authors would like to thank Dr. Bryan McCranor for his scientific insight, Ms. Robyn Lee for her statistical analyses and guidance, and CPT Sabrina McGraw, Ms. Robin Deckert, Dr. Dorian Olivera, and Ms. Jannitt Simons for their scientific, technical, and administrative assistance throughout the project. RL, JT, KS, and JA were supported in part by appointments to the Research Participation Program for the U.S. Army Medical Research and Materiel Command administered by the Oak Ridge Institute for Science and Education through an agreement between the U.S. Department of Energy and U.S. Army Medical Research and Materiel Command.

Grants

This work was supported by an interagency agreement between the National Institutes of Health/National Institute of Allergy and Infectious Diseases (NIH/NIAID) and USAMRICD (“Chemicals Affecting the Respiratory Tract – Pulmonary Toxicant Gases” IAA# AOD16027–001-00000).

Abbreviations

CEE	Calculated exposure equivalent, mg/kg
Ct	Concentration time product
f, f_n	Respiratory frequency, breaths/min; normalized respiratory frequency
$\mathbf{LCt_{50}}$	Lethal exposure concentration-time product for 50% of the population
MV, $\mathbf{MV_n}$	Minute Volume, mL/min; normalized minute volume
t, t_n	Time elapsed since exposure start, min; normalized elapsed time
t_{exp}	Length of time of the exposure period, min

t_{TOD}, t_{TODn}	Time of death, min; normalized time of death
TEM	Transmission electron microscopy
TIC	Toxic industrial chemical
TV, TV_n	Tidal Volume, mL/breath; normalized tidal volume
PCA	Principal component analysis
PH_3	Phosphine

References

Anand R, Binukumar BK, Gill KD. 2011 Aluminum phosphide poisoning: an unsolved riddle. Journal of Applied Toxicology. 8;31:499–505. [PubMed: 21607993]

Barbosa A, Rosinova E, Dempsey J, Bonin A. 1994 Determination of genotoxic and other effects in mice following short term repeated-dose and subchronic inhalation exposure to phosphine. Environ Mol Mutagen.24:81–88. [PubMed: 7925330]

Berners-Price SJ, Sadler PJ. 1988 Phosphines and metal phosphine complexes: relationship of chemistry to anticancer and other biological activity In: Bioinorganic Chemistry. Springer p. 27–102.

Bogle RG, Theron P, Brooks P, Dargan PI, Redhead J. 2006 Aluminium phosphide poisoning. Emerg Med J. 1;23:e3. [PubMed: 16373788]

Burgess J 2001 Phosphine exposure from a methamphetamine laboratory investigation. Journal of toxicology Clinical toxicology.39:165. [PubMed: 11407503]

Cavasin R, DePalo M, Tumambing J. Updates on the global application of Eco2Fume and Vaporph3OS® phosphine fumigants. Proceedings of the 9th International Working Conference on Stored Product Protection; 2006 15 to 18 October 2006.

Chefurka W, Kashi KP, Bond EJ. 1976 The effect of phosphine on electron transport in mitochondria. Pesticide Biochemistry and Physiology.6:65–84.

Cheng Q, Valmas N, Reilly PEB, Collins PJ, Kopittke R, Ebert PR. 2003 Caenorhabditis elegans Mutants Resistant to Phosphine Toxicity Show Increased Longevity and Cross-Resistance to the Synergistic Action of Oxygen. Toxicological Sciences. May 1, 2003;73:60–65. [PubMed: 12700416]

Dua R, Gill KD. 2004 Effect of aluminium phosphide exposure on kinetic properties of cytochrome oxidase and mitochondrial energy metabolism in rat brain. Biochim Biophys Acta. Sep 6;1674:4–11. Epub 2004/09/03. [PubMed: 15342109]

Flury F 1921 Über kampfgasvergiftungen I. Über reizgase. Research in Experimental Medicine.13:1–15.

Haber F 1924 Zur geschichte des gaskrieges In: Fünf Vorträge aus den jahren 1920–1923. Springer p. 76–92.

Jian F, Jayas DS, White ND. 2000 Toxic action of phosphine on the adults of copra mite Tyrophagus putrescentiae [Astigmata: Acaridae]. Phytoprotection.81:23–28.

Kligerman A, Bishop J, Erexson G, Price H, O'Connor R, Morgan D, Zeiger E. 1994 Cytogenetic and germ cell effects of phosphine inhalation by rodents: II. Subacute exposures to rats and mice. Environ Mol Mutagen.24:301–306. [PubMed: 7851342]

Mehrpour O, Jafarzadeh M, Abdollahi M. 2012 A systematic review of aluminium phosphide poisoning. Arh Hig Rada Toksikol. 3;63:61–73. [PubMed: 22450207]

Mioduszewski R, Manthei J, Way R, Burnett D, Gaviola B, Muse W, Thomson S, Sommerville D, Crosier R. 2002 Interaction of Exposure Concentration and Duration in Determining Acute Toxic Effects of Sarin Vapor in Rats. Toxicological Sciences.66:176–184. [PubMed: 11896284]

Murli H 1991 Mutagenicity Test on Phosphine: Measuring Chromosomal Aberration Frequencies in Cultured Rat Whole Blood Lymphocytes. Contract study by Hazleton Laboratories of America, Inc Study.444.

Muthu M, Krishnakumari M, Majumder S. 1980 A study on the acute inhalation toxicity of phosphine to albino rats. B Environ Contam Tox.24:404–410.

Nakakita H 1987 The Mode of Action of Phosphine. J Pestic Sci.12:299–309.

Nath NS, Bhattacharya I, Tuck AG, Schlipalius DI, Ebert PR. 2011 Mechanisms of phosphine toxicity. J Toxicol.2011:494168. [PubMed: 21776261]

Newton PE, Schroeder RE, Sullivan JB, Busey WM, Banas DA. 1993 Inhalation toxicity of phosphine in the rat: Acute, subchronic, and developmental. Inhalation Toxicology.5:223–239.

Pauluhn J 2014 Time Scaling of Dose and Time to Response: The Toxic Load Exponent In: Inhalation Toxicology. 3rd ed.: CRC Press p. 121–136.

Perkins MW, Wong B, Olivera D, Sciuto AM. 2015 Phosphine In: Hamilton and Hardy's Industrial Toxicology. Hoboken, NJ: Wiley.

Perkins MW, Wong B, Rodriguez A, Devorak J, Sciuto AM. 2015 Measurement of various respiratory dynamics parameters following acute inhalational exposure to soman vapor in conscious rats. Inhal Toxicol.27:432–439. Epub 2015/07/25. [PubMed: 26207672]

Perkins MW, Wong B, Tressler J, Rodriguez A, Sherman K, Andres J, Devorak J, L. Wilkins W, Sciuto AM 2017 Adverse respiratory effects in rats following inhalation exposure to ammonia: respiratory dynamics and histopathology. Inhalation Toxicology. 2017/01/02;29:32–41. [PubMed: 28183203]

Proudfoot AT. 2009 Aluminium and zinc phosphide poisoning. Clin Toxicol (Phila). 2;47:89–100. [PubMed: 19280425]

Raina A, Shrivastava HC, Mathur N, Dogra TD. 2003 Validation of qualitative test for phosphine gas in human tissues. Indian J Exp Biol. 8;41:909–911. [PubMed: 15248495]

Reeve I 2014 Estimation of exposure to persons in California to phosphine due to use of aluminum phosphide, magnesium phosphide, and cylinderized phosphine gas California Environmental Protection Agency, Department of Pesticide Regulation, Sacramento, CA.

Ryan RF, De Lima C. 2014 Phosphine-an overview of a unique 80 year fumigant. General and Applied Entomology: The Journal of the Entomological Society of New South Wales.42:31.

Sciuto AM, Wong BJ, Martens ME, Hoard-Fruchey H, Perkins MW. 2016 Phosphine toxicity: a story of disrupted mitochondrial metabolism. Annals of the New York Academy of Sciences. 6;1374:41–51. [PubMed: 27219283]

Singh S, Bhalla A, Verma SK, Kaur A, Gill K. 2006 Cytochrome-c oxidase inhibition in 26 aluminum phosphide poisoned patients. Clinical Toxicology.44:155–158. [PubMed: 16615671]

Ten Berge W, van Heemst MV. Validity and accuracy of a commonly used toxicity-assessment model in risk analysis. Proceedings of the IChemE Symposium Series; 1983.

Ten Berge W, Zwart A, Appelman L. 1986 Concentration—time mortality response relationship of irritant and systemically acting vapours and gases. Journal of Hazardous Materials.13:301–309.

Tumambing J, Depalo M, Garnier JP, Mallari R. Eco2Fume and Vaporph3OS® phosphine fumigants - global application updates. Proceedings of the Proceedings of the 9th International Conference on Controlled Atmosphere and Fumigation in Stored Products; 2012.

Wang Y, Lew K-K, Ho T-T, Pan L, Novak SW, Dickey EC, Redwing JM, Mayer TS. 2005 Use of Phosphine as an n-Type Dopant Source for Vapor−Liquid−Solid Growth of Silicon Nanowires. Nano Letters. 2005/11/01;5:2139–2143. [PubMed: 16277441]

WARITZ RS, BROWN RM 1975 Acute and subacute inhalation toxicities of phosphine, phenylphosphine and triphenylphosphine. The American Industrial Hygiene Association Journal. 36:452–458. [PubMed: 1229887]

Willers-Russo LJ. 1999 Three fatalities involving phosphine gas, produced as a result of methamphetamine manufacturing. Journal of Forensic Science.44:647–652.

Winks R 1982 The toxicity of phosphine to adults of Tribolium castaneum (Herbst): time as a response factor. Journal of Stored Products Research.18:159–169.

Winks R 1984 The toxicity of phosphine to adults of Tribolium castaneum (Herbst): time as a dosage factor. Journal of Stored Products Research.20:45–56.

Winks R 1986 The biological efficacy of fumigants: time/dose response phenomena. Pesticides and humid tropical grain storage system.211–221.

Witschi H 1999 Some notes on the history of Haber's law. Toxicological Sciences.50:164–168. [PubMed: 10478852]

Wong B, Perkins MW, Santos MD, Rodriguez AM, Murphy G, Sciuto AM. 2013. Development of a model for nerve agent inhalation in conscious rats. Toxicol Mech Methods. 9;23:537–547. Epub 2013/04/16. [PubMed: 23581557]

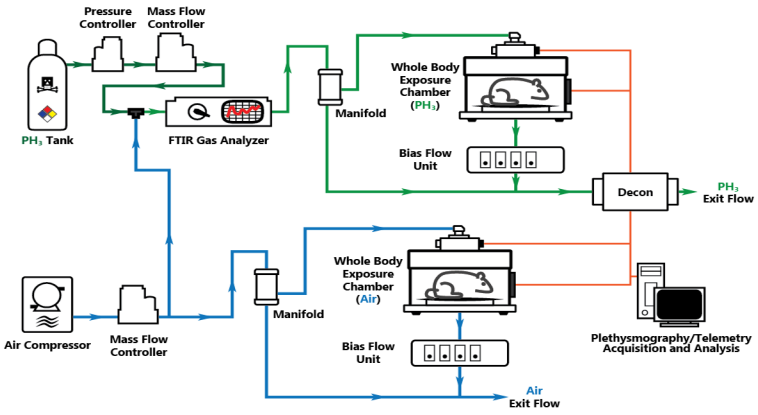

Fig. 1. – Exposure System Schematic

Configuration of the dynamic exposure system with integrated real-time physiological monitoring capabilities used to expose conscious, unrestrained animals to phosphine gas.

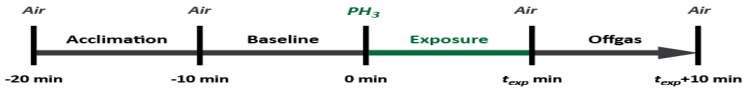

Fig. 2. – Inhalation Exposure Paradigm

For all inhalation exposures, animals were individually placed into WBP chambers at $t = -20$ min for acclimation until $t = -10$ min, at which point the recording of respiratory dynamics was initiated. At $t = 0$ min, flow of the PH_3 gas mixture into each exposure chamber began and continued for 10 to 40 min (t_{exp}). At $t = t_{exp}$, the flow of the PH_3 gas mixture into the WBP ceased. Animals remained in the WBP for an additional 10 min for off-gassing, observation, and data recording. At $t = t_{exp}+10$ min, surviving animals were removed from the inhalation exposure system.

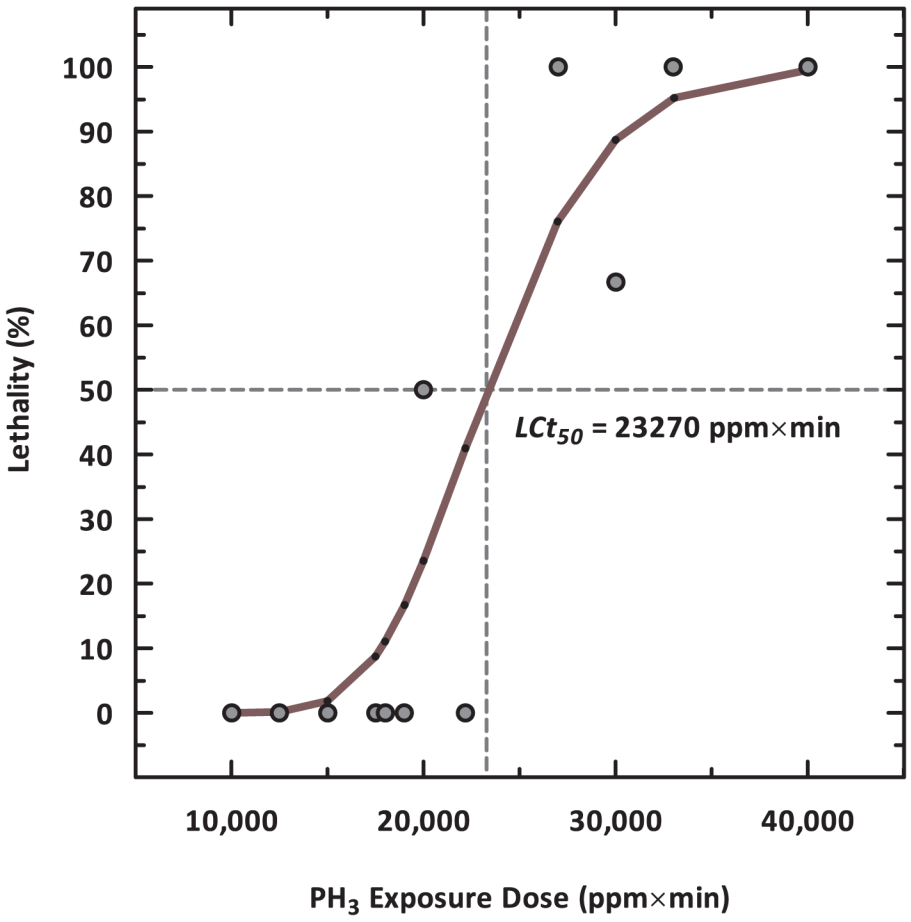

Fig. 3. – Lethality of Inhaled Phosphine

Lethality of inhaled PH_3 in rats at 24 hr post-exposure, as determined by probit analysis. The filled circles are the experimental data (Supplemental Material , Table 3 – Probit Analysis Development), and the line is the fitted curve.

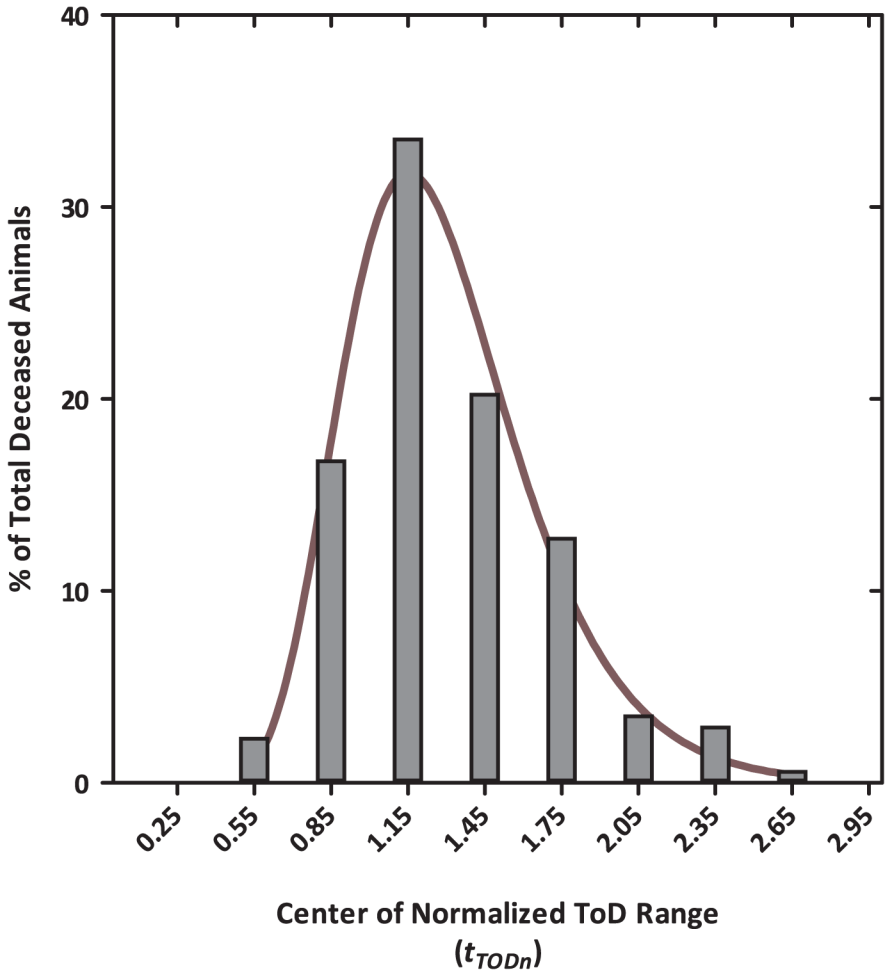

Fig. 4. – Time-of-Death Distribution

The time-of-death distribution shows the percentage of deceased animals that died from PH_3 exposure during a given normalized time-of-death ($t_{TODn} = t_{TOD}/t_{exp}$) range. For each bar, the abscissa is the center of the t_{TODn} range, with the width of each bin set at 0.3, and the ordinate set as the percentage of deceased animals that died within its range, with the total number of deceased animals being 167. A total of 9 animals died after $t_n = 3.1$ and are not shown.

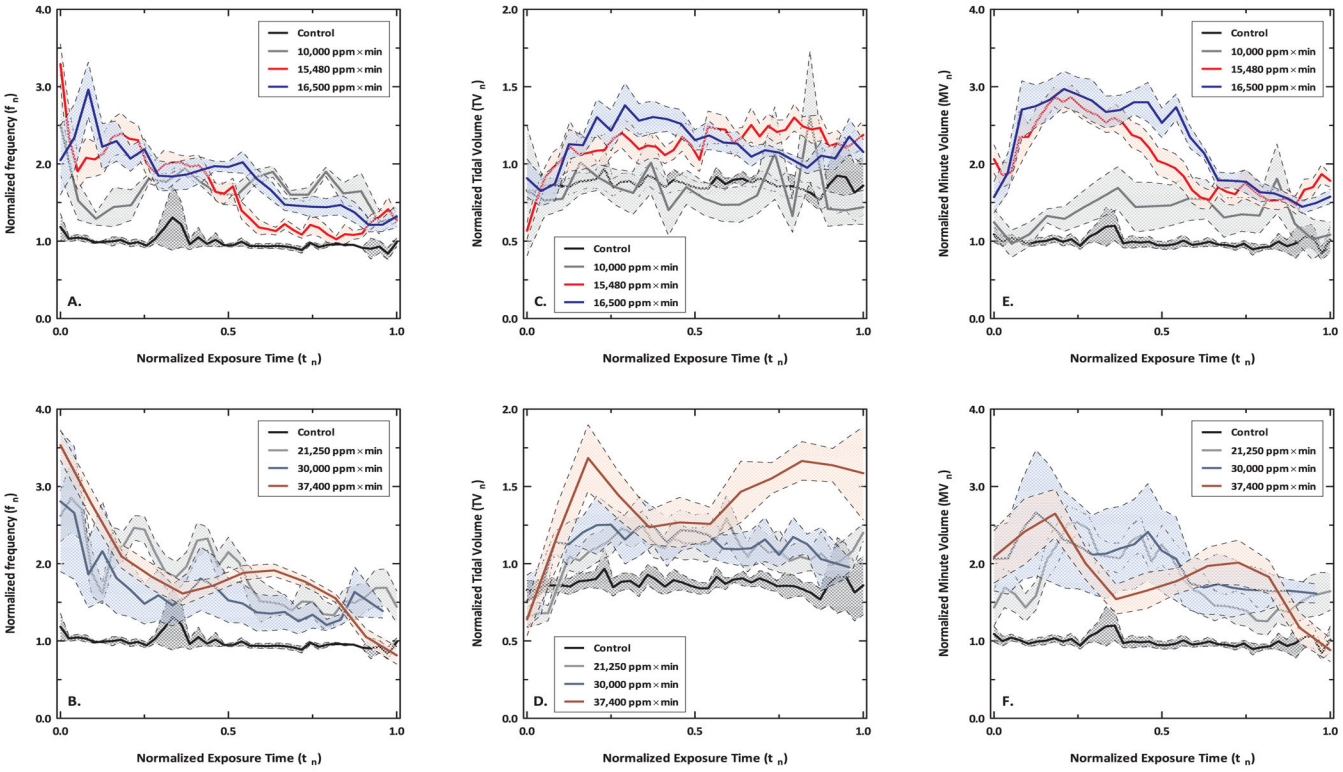

Fig. 5. – Respiratory Dynamics during Exposure to Phosphine Gas

All graphs show normalized parameters of respiratory function versus normalized exposure time. For each trace, N = 4–6 and error bands are shown as ± SEM. A,B) Normalized respiratory frequency (f_n) for lower and higher phosphine doses, respectively. C,D) Normalized tidal volume (TV_n) for lower and higher phosphine doses, respectively. E,F) Normalized minute volume (MV_n) for lower and higher phosphine doses, respectively.

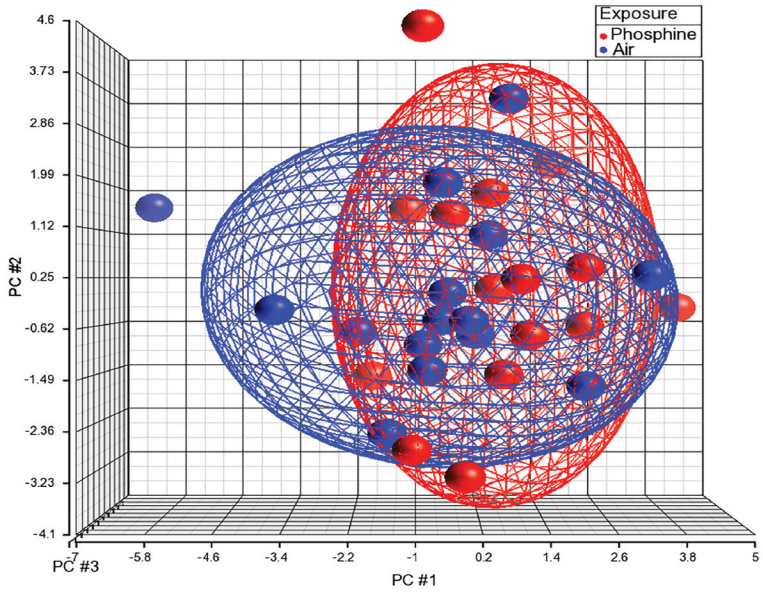

Fig. 6. – Principal Component Analysis of Cardiac Tissue

Points on the PCA group by similarity where those points close in proximity share more similarities than points grouped farther away. Each point on the pot represents one sample in the dataset derived from cardiac tissue. Cardiac samples from phosphine-exposed (15,480 ppm×min) animals are shown in red, and air control samples are shown in blue. The PCA describes 72.5% of the variability in the data set (PC #1 32.6%; PC #2 25.3%; PC #3 14.6%).

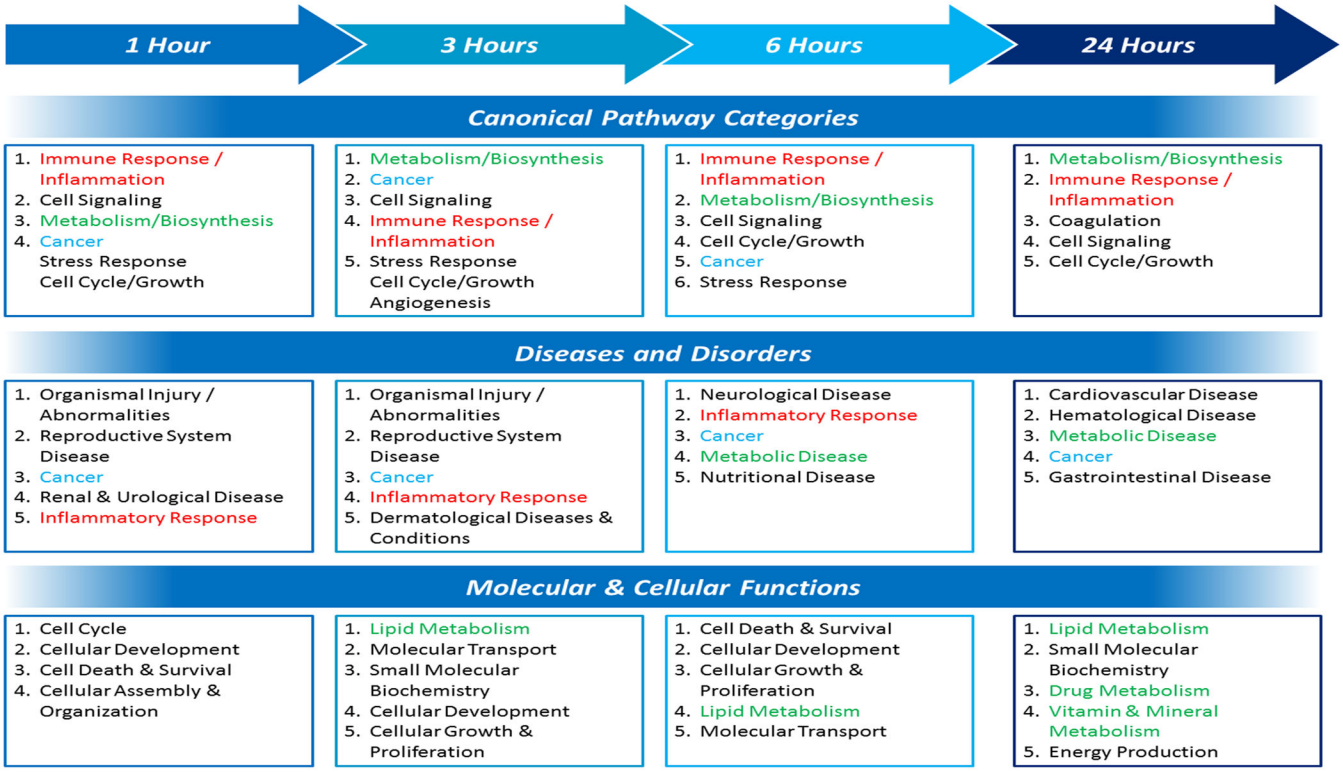

Fig. 7. – Pathway Analysis of Phosphine-Induced Gene Expression Changes in Cardiac Tissue (15,480 ppm×min)

Significant canonical pathways were grouped into functional categories and ranked according to number of canonical pathways within the category. Inflammation/immune response is shown in red, cancer in blue, and metabolism in green.

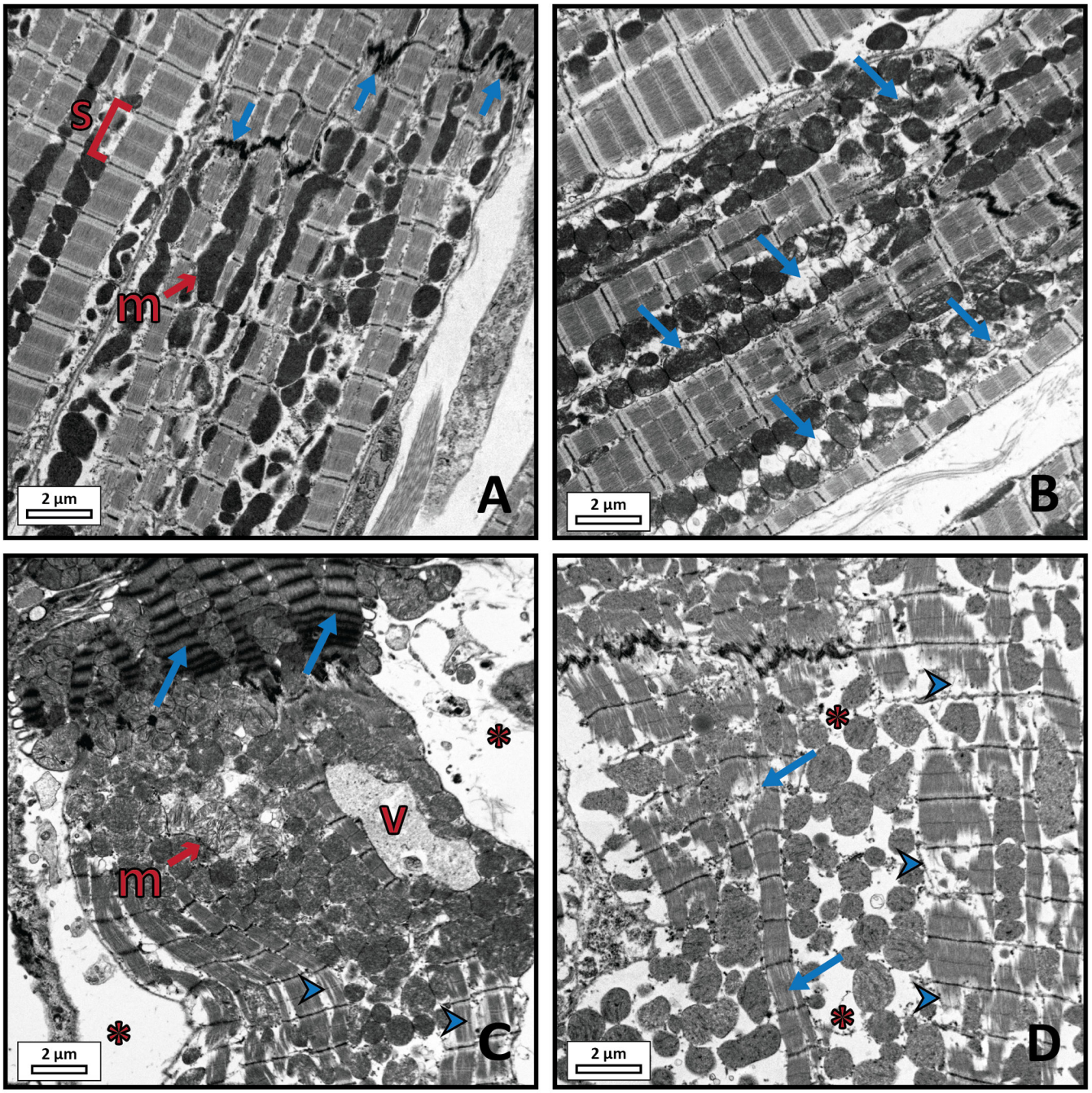

Fig. 8. – Transmission Electron Microscopy of Cardiac Tissue

A) Cardiac myofibers from left ventricle of 6 hr post-exposure time matched control animal showing normal ultrastructure; mitochondria (m), intercalated disc (arrow), sarcomere (s). B) Cardiac myofiber from left ventricle at 3 hr post-exposure showing edematous intermyofibrillar mitochondria with swollen and lysed cristae (arrow). C) Degenerated cardiac myofiber from left ventricle at 6 hr post-exposure showing loss of sarcomere striation patterns (arrow) adjoining a second myofiber showing loss of myofilaments (arrowheads), swollen mitochondria (m), formation of a large intermyofibrillar vacuole (v),

and edematous endomysium (asterisk). D) Degenerating cardiac myofiber from left ventricle at 6 hr post-exposure showing loss of sarcomere striation patterns (arrow), loss of myofibrils (arrowhead), and intermyofibrillar edema (asterisk).

Table 1

– Empirical Data for Equivalent Endpoint Analysis

Dose ppm×min	Agent Concentration mg/m^3	Exposure Time min	Average Animal Mass g	CEE (Experimental)† mg/kg
0*	0	40	316.5	0
10,000	695	20	323.0	6.145
15,480	538	40	323.0	14.641
16,500	917	25	327.2	16.760
21,250	917	33	329.5	17.796
30,000	1390	25	338.7	20.115
37,400	4726	12	321.5	41.621

*Not included in the nonlinear least squares regression

†Calculated from respiratory data using Equation 1

Table 2

– Baseline Values for Respiratory Dynamics Parameters

Parameter		Control Average ± SD	
Frequency	(f)	110 ± 29	breaths/min
Tidal Volume	(TV)	0.88 ± 0.09	mL
Minute Volume	(MV)	107 ± 18	mL/min